K. Mitsuda

Temperature Dependence of Ginga Clock Rate

J. Deeter

University of Washington

宇宙研, 昭和 63.11.28

- - - - - - - - - - - - - - - - - -

Outline of Text

Introduction

1. Determination of clock rate.
   (a) Comparision made with clock at KSC every contact orbit.
   (b) Correction is made for satellite range (~8 ms).
   (c) Time difference between two consecutive comparisions is divided by number of clock cycles to get the mean clock period (nominally 8 sec).
   (d) Time history of a sample of data given in Fig. 1.

2. Determination of clock temperature.
   (a) Many temperature sensors in satellite.
      -- temperature recorded every 8, 64, 256 sec, depending on recording rate.
      -- temperature recorded in approximately 0.5^{o} steps.
   (b) Location of sensors -- CP-4 is closest to DP unit.
   (c) Time history of CP-4 given in Fig. 2, over same data interval as Fig. 1.

3. Clock period-temperature correlations.
   (a) Period vs. CP-4 temperature given in Fig. 3.
       -- note the rapid turn-over in the relationship near 18° C, complicating the use of the correlation for converting temperature into clock rate.
   (b) Better correlation is obtained by using a linear combination of several sensors (CP-4, BDR, CP-1, and BP-4), shown in Fig. 4.
   (c) Emperical temperature-clock rate function is determined by averaging both variables in 0.5° intervals spaced every 0.25°, as shown in Fig. 5.
   (d) Temperature averaged over each satellite orbit, converted into clock period using Fig. 5, and plotted in Fig. 6 to compare with measured periods (shown in Fig. 1).

4. Recovery of clock phase from temperature data.
   (a) Clock rate inferred from satellite temperature is integrated to obtain an estimate of clock phase.
   (b) Actual clock measurements are compared with the temperature inferred phase; the results are shown in Fig. 7, and the difference between the two quantities is shown in Fig. 8.
   (c) Day-night cycle in satellite temperature (Fig. 9), induces a possible 1-ms term in the clock phase (Fig. 10.)
       -- side effect is an error term with similar magnitude when temperature is not averaged uniformly over the day-night cycle.
   (d) Clock measurements compared with the temperature corrected for incomplete day-night sampling is shown in Fig. 11, and the residuals in Fig. 12.

5. Discussion
   (a) Clock rate dependence on temperature is strange and unexpected.
   (b) Improvements in the analysis are necessary before the temperature can be used as a good indicator of the clock rate:
       -- better computation of average temperature over the day-night cycle for the data used in the correlation diagrams;
       -- investigation into whether there is a time delay between nearby temperatures and the actual temperature of the clock.
   (c) Further investigation needed into whether the clock feels the full effect of the day-night cycle
       -- study the timing of a rapid, bright pulsar such as Crab pulsar.

Introduction

For high-flux, short-period X-ray pulsars such as SMC X-1 and Her X-1, we expect to obtain very accurate pulse timing using Ginga LAC data, achieving an error of less than 1 ms in an observing time of less than one hour duration. It is therefore important that the phase of the satellite clock be known to a precision of better than 1 ms in order to obtain full use of the pulse-timing data. The present study was initiated to find out whether the Ginga clock is sufficiently stable to rely on the convenient method of using an average clock rate between consecutive comparisions of the satellite clock with the clock at KSC ground station. If this is not the case, it is then important to find a method of correcting the clock rate if possible. Being able to verify the actual clock rate is particularly important for the remote (non-contact) orbits, for which there are intervals of 16 hours (usually) and even 40 hours (across Sunday vacations) for which there is no comparision with the KSC clock.

It was quickly discovered that there was a large variation in the clock rate of about 1 part in 10^6. It was suspected that this variation was due mainly to changes in the satellite temperature. This suspicion was confirmed by constructing a correlation diagram of clock rate versus temperature. However, it was discovered that the relationship between clock rate and temperature is not even approximately linear in the range of satellite operating temperatures, but is strongly peaked near 18° C. This unexpected behavior greatly complicates any effort to use the temperature data to correct the clock rate between comparisions with the clock at KSC.

However, some success was achieved in recovering the clock phase from the temperature data. Using an emperical relation between for clock rate as a function of temperature, the time history of temperature can be converted to a time history of the clock rate. This derived clock rate can then be integrated to give the clock phase at much closer spacing than is provided by the direct comparision with a clock at the KSC ground station. Much of the overall clock behavior is recovered by this method. For instance, in a 12-day test interval, the true clock phase drifts by ± 60 ms from that of a constant clock, and the temperature derived clock phase follows the true clock phase within ± 10 ms.

This is a pretty good result, considering that not too much care was taken in the present analysis in computing the emperical relationship between temperature and clock rate. Methods for improving the analysis are now being considered. For instance, there is a definite day-night cycle in the satellite temperature. This cycle becomes important in constructing the emperical relationship to the extent that sometimes the temperature is averaged only over a portion

of the day-night cycle, while the clock rate is always averaged over a full day-night cycle. Removing this mismatch in sampling may improve the reliability of the emperical relationship between temperature and clock rate. A second improvement would be to use a smooth interpolation curve rather than the collection of straight-line segments currently employed. A third possibility is to correct for a time delay between the temperature of the satellite (outside the data processor) and the temperature of the clock circuit (inside the DP). With these improvements, it may be possible to recover the clock phase to an accuracy of 2-3 ms during the remote passes, which would be a significant improvement over the 10 ms recovery presently achieved, and the 10 ms deviations in phase from a constant clock rate.

1. Determination of Clock Rate

A clock marker is inserted into the Ginga data stream every 8 sec, along with a running cycle count. This clock marker in the real time data is compared to a clock at the KSC ground station at the beginning of every contact pass. The time of comparision is corrected for light transit time from the satellite (about 8 ms), to yield the time of generation. The average clock period is obtained by dividing successive times of generation by the number of intervening clock cycles (there are approximately 750 clock cycles between comparisions on consecutive orbits). This period is always within a few μs of 8 sec, and provides a basis for assigning time of observation to the data by linear interpolation between successive clock comparisions.

In order to verify the stability of the clock rate, the clock period was computed for a segment of data approximately 20 days in duration. The results of this computation are shown in Figure 1. It can be seen that the clock period drifts by at least 10 μs from the nominal value of 8 sec, and that this drift can be quite rapid with large drifts occuring within the space of a few hours. It was suspected that a major portion of this variation in clock rate was due to temperature variations in the clock circuit, and so the next indicated step was to investigate the temperature variations in the satellite.

2. Determination of Clock Temperature

There are over 50 temperature sensors in the Ginga satellite, each of which is sampled every 8, 64, or 256 sec depending on the data mode. Most of these temperatures are recorded in only 0.5° steps. This low recording resolution is not a serious drawback, because there is a fairly large number of measurements which can be averaged.

The sensors which were used in this analysis are BDR (bubble data recorder); CP-1, CP-3, and CP-4 (on center panels 1, 3, and 4, respectively); and BP-3 and BP-4 (on the inside and outside surfaces of the base panel, respectively). The sensors closest to the DP (data processer, within which the clock circuit is mounted) are CP-4 (just above the DP) and BDR (just below the DP). Unfortunately there is no temperature sensor within the DP itself.

The time history of the temperature from the CP-4 sensor is shown in Figure 2, for the same interval used in Figure 1. It is apparent that the excursions in CP-4 temperature have a total range of nearly 5^{o}, and that the variations are somewhat correlated with the varitions in period shown in Figure 1. The next step is to study the relationship between the clock rate and the temperature given by a nearby sensor.

3. Clock rate -- Temperature Correlations

The relationship beteen clock rate and temperature of the CP-4 sensor is shown in Figure 3 for a time interval approximately 75 days long, from 1988 July 20 to 1988 October 5. During this interval the clock period ranged from 8 sec minus 15 μs to 8 sec plus 6 μs, while the CP-4 temperature ranged from 13.5^{o} to 20^{o} C. This relationship is shown in Figure 4. It is clear that the relationship is far from linear, having a fairly sharp maximum near 18^{o} C. The relationship also exhibits a larger scatter that expected from the error bars assigned on the basis of a 0.5 ms uncertainty in every determination of the time of the satellite clock.

Some of the scatter is likely due to uncertainty in the determination of the temperature. For instance there may be a large systematic error because the CP-4 sensor is not inside the DP and hence does not necessarily reflect the exact temperature of the clock circuit. It is possible that a linear combination of sensors whould better reflect the temperature of the clock circuit than does CP-4 itself, and thereby reduce the scatter seen in Figure 3. To keep this analysis simple, only a portion of data was used, restricted to the range of CP-4 temperature less than 18^{o} and clock period less than 8 sec where the clock dependence on temperature is apparently linear. Intially the regression was performed on all six temperatures mentioned in Section 2 (plus a constant temperature to allow for a nonzero intercept), but it was found that BP-3 and CP-3 had coefficients close to zero. They were therefore deleted, and the regression was repeated on the other four temperatures, again including a constant temperature to allow for nonzero intercept.

Table 1.
Coefficients from Regression of Clock Period
on the Temperature Indicated by Four Sensors
Near the Ginga Data Processor

Sensor Name	Regression Coefficent (μs/ ^{o}C)	Normalized Coefficient
BDR	1.2929	0.4308
CP-4	2.7118	0.9036
BP-4	0.3401	0.1133
CP-1	-1.3437	-0.4477

The coefficients from this regression are shown in Table 1, together with the "normalized" coefficents which sum to unity and therefore represent a good approximation to a synthesized temperature of the clock. The rms scatter in the clock period for this regression is 0.886 μs, compared to 1.176 μs for the regression on CP-4 and a constant temperature. The minimum rms scatter, based on just the 1 ms precision of the clock comparision, is roughly 0.5 μs.

The correlation between the clock period and the combination temperature is shown in Figure 4. The correlation is tighter than it is for CP-4 alone, not only at low temperatures were the regression was performed, but also at high temperatures as well.

The next part of this investigation is to determine whether the clock period - temperature relationship can be used as a practical tool for recovering the local clock rate, and from that, the local clock phase by integration. The relationship seen in Figure 4 is so peaked that it will not be fit very well by a low-degree polynomial. It was therefore decided to approximate the relationship numerically by forming normal points. Intermediate values can then be obtained by interpolation. The normal points were formed by averaging the clock period and the combined temperature in 0.5^{o} steps, spaced every 0.25^{o}. This overlapping of bins makes a smoother function than would independent bins spaced every 0.5^{o}. The resulting relationship is shown in Figure 5.

As a check on the reliability of this conversion of temperature into clock rate, a direct check of synthesized period with actual periods (see Fig. 1) for the critical interval from 1988 August 23 to 1988 September 3. (This interval includes a passage back and forth across the maximum in the relationship.) The converted temperature was averaged in 10-minute bins, corrected for a day-night temperature variation (discussed below), transformed into clock period,

and then averaged by satellite orbit (approximately 97 min.). This allows a fairly direct check against the measured clock periods, as shown in Figure 6. The synthesized temperatues are generally consistent with the direct measurements, with only one point deviating by as much as 2 σ.

4. Recovery of Clock Phase from Temperature Data

The temperature-inferred clock rate is integrated with respect to time to obtain the temperature clock phase as a function of time. There is of course an constant of integration which can be assigned to make the integrated curve match the actual measurements as closely as possible. For the time being, no care was taken in choosing this constant of integration, since the match is not particularly good. A portion of this comparision is shown in Figure 7. For this figure, the combined temperature was averaged every 10 minutes, and integrated without removing the day-night variation in the temperature. Wherever there was a gap in the data stream (i.e., when the data recorder was turned off), the temperature was interpolated across the gap.

The overall behavior of the temperature-inferred clock phase follows the measured clock phase, but there are disagreements in details. The differences are shown better in Figure 8, where the clock period is interpolated linearly between consecutive comparisions of the clock with the ground station, and the resulting piece-wise linear clock phase is subtracted from the temperature-inferred clock phase. The locations of the clock comparisions are indicated by symbols at a phase difference of zero, while the line indicate the difference between the temperature-inferred phase and the piece-wise linear phase from the clock measurements. The excursions with large curvature seen in Figure 8 are generally caused by a change in clock rate due to a change in the temperature, and are actually the kind of behavior that this analysis is intended to recover. The success of the analysis rests to a large extent on confidence that the temperature dependence is modeled well, which can be verified by the agreement of the two phase determination at the actual clock comparisions.

The agreement of the two determinations of clock phase is not perfect, as there are sometimes fairly large phase drifts (up to 10 ms) across the remote orbits. One source of phase drift was thought possibly to arise from incomplete sampling of the day-night temperature cycle, as shown in Figure 9. This variation is important, because it can introduce as large as a 0.5 ms term in the clock phase, as shown in Figure 10. The day-night temperature variation was found to closely follow the formula

$$\Delta T = -0.608 \cos 2\pi (t - 47395.9192)/0.0669048,$$

(t in MJD), for the interval 1988 August 22 to 1988 September 3. The above temperature variation was subtracted

from the 10 minute average combined temperature prior to conversion to clock rate. The resulting clock phase is shown in Figure 11, and the difference from the piece-wise linear phase is shown in Figure 12. There is no obvious improvement over the results given in Figures 7 and 8, which contain no correction for the day-night temperature variation. This result indicates that the temperature data usually samples the day-night cycle fairly well.

5. Discussion

The period of the Ginga clock has a strange temperature dependence, which is very much non-linear and complicates any attempt to correct the clock phase to millisecond accuracy. It is very unfortunate that this defect was not detected prior to launching the satellite. The only laboratory check made on the clock rate was at intervals of 10° C, which was not adequate to disclose the sharp maximum in clock period near 20° C.

Some improvements are necessary in the analysis procedure before it will be completely useful for providing the clock phase during remote orbits. For instance, the day-night variation should be removed from the temperature data use in the correlation diagram, and this procedure could provide a tighter correlation between clock rate and temperature. A second improvement would be to use a more accurate method for the numerical relationship between clock rate and temperature than linear interpolation on normal points. Additional improvement might result by considering a time delay between satellite temperatures measured outside the data processor and the temperatue of the clock, inside the DP.

Finally, as a separate problem, investigation is needed into the question of whether the clock feels the full effect of the day-night temperature cycle, some 0.6° in amplitude. As seen in Figure 9, this cycle could induce a 0.5 ms term in the clock phase, and this will be an important effect for timing pulsars at the sub-millisecond level. The obvious choice for this analysis is a rapid, bright X-ray pulsar (such as the Crab pulsar). So far this investigation has not been started.

Figure Captions

Fig. 1. Ginga clock period (minus 8 sec) as a function of time, for the interval 1988.8.19 to 1988.9.6. Error bars are based on a 0.5 ms uncertainty in each clock measurement, a limitation due to the recording of the time comparision to only 1 ms.

Fig. 2. Temperature of CP-4 sensor as a function of time, for the interval 1988.8.19 to 1988.9.6. Errors in the data points are roughly the size of the symbols.

Fig. 3. Correlation diagram of Ginga clock period (minus 8 sec) versus temperature of CP-4, for the interval 1988.7.20 to 1988.10.4.

Fig. 4. Correlation diagram of Ginga clock period (minus 8 sec) versus a linear combination of temperatures from sensors BDR, CP-4, CP-1, and BP-4, for the interval 1988.7.20 to 1988.10.4 (see also Table 1 in the text).

Fig. 5. Normal points for the clock period - temperature relationship, based on the data shown in Fig. 4.

Fig. 6. Clock period (minus 8 sec) inferred from satellite temperature (line) compared to the measured clock period (diagonal crosses), for the interval 1988.8.23 to 1988.9.3.

Fig. 7. Clock phase inferred from satellite temperature (line) compared to measured clock phase (crosses), for the interval 1988.8.23 to 1988.9.3 (no correction for day-night temperature cycle).

Fig. 8. Difference between the clock phase inferred from satellite temperature and the phase obtained from linear interpolation between clock measurements, for the interval 1988.8.22 to 1988.9.3 (based on data in Fig. 7, again with no correction for day-night temperature cycle). The crosses at zero phase represent the times of actual clock measurements.

Fig. 9. Temperature variation of sensor CP-4, showing the day-night temperature cycle (about 15 cycles per day), for the interval 1988.8.26 to 1988.8.28. The line segments connect successive 10-minute averages.

Fig. 10. Clock phase based on integrating the temperature-inferred clock rate, showing the possible effect of day-night temperature cycle, for the interval 1988.8.26 to 1988.8.28. This figure is much like Fig. 8, with the line segments giving the difference between the temperature-inferred clock phase and the phase obtained from linear interpolation between successive clock measurements. The crosses at zero phase indicate the times of actual clock measurements.

Fig. 11. Clock phase inferred from satellite temperature (line) compared to measured clock phase (crosses), for the interval 1988.8.23 to 1988.9.3 (correction for day-night temperature cycle has been applied).

Fig. 12. Difference between the clock phase inferred from satellite temperature and the phase obtained from linear interpolation between clock measurements, for the interval 1988.8.22 to 1988.9.3 (based on data in Fig. 7, again with a correction for the day-night temperature cycle). The crosses at zero phase represent the times of actual clock measurements.

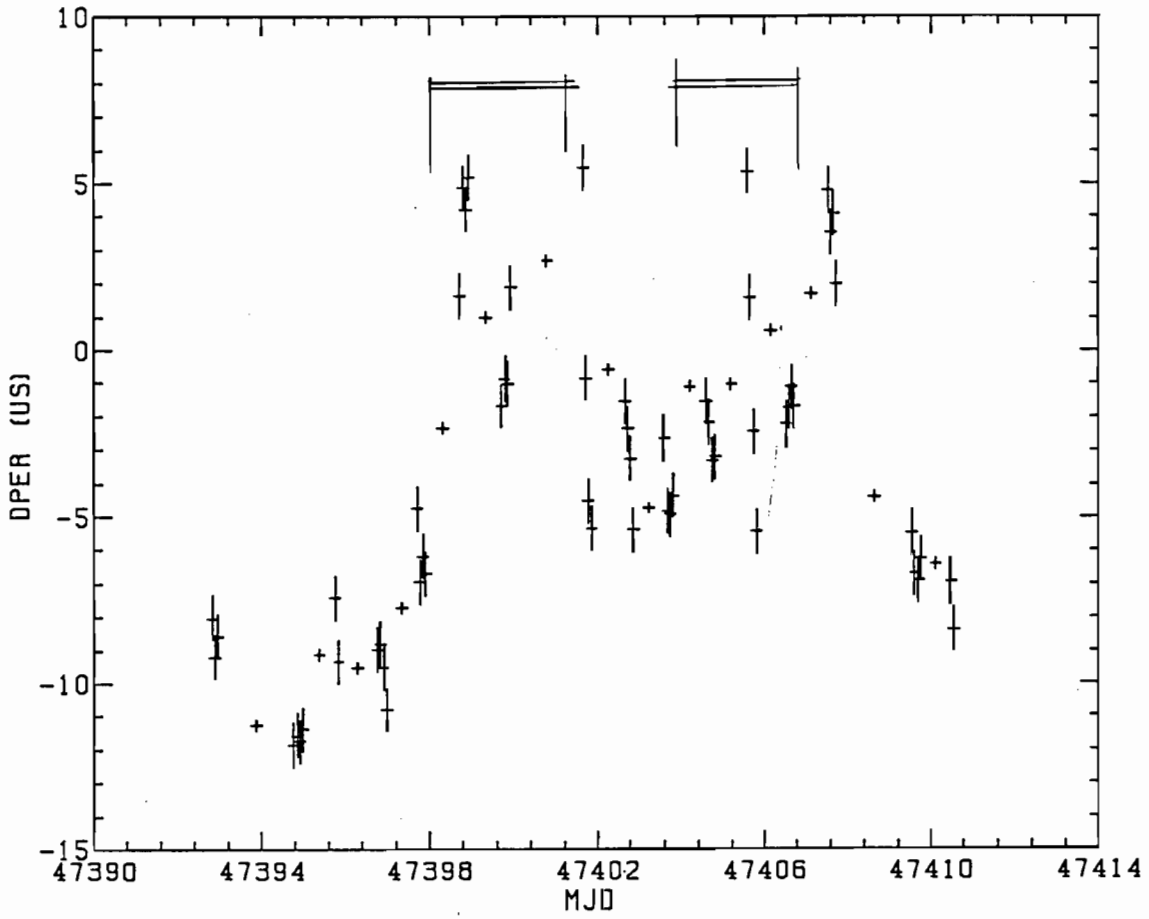
10
5
0
-5
-10
-15
DPER (US)
47390
47394
47398
47402
47406
47410
47414
MJD

Fig. 1.

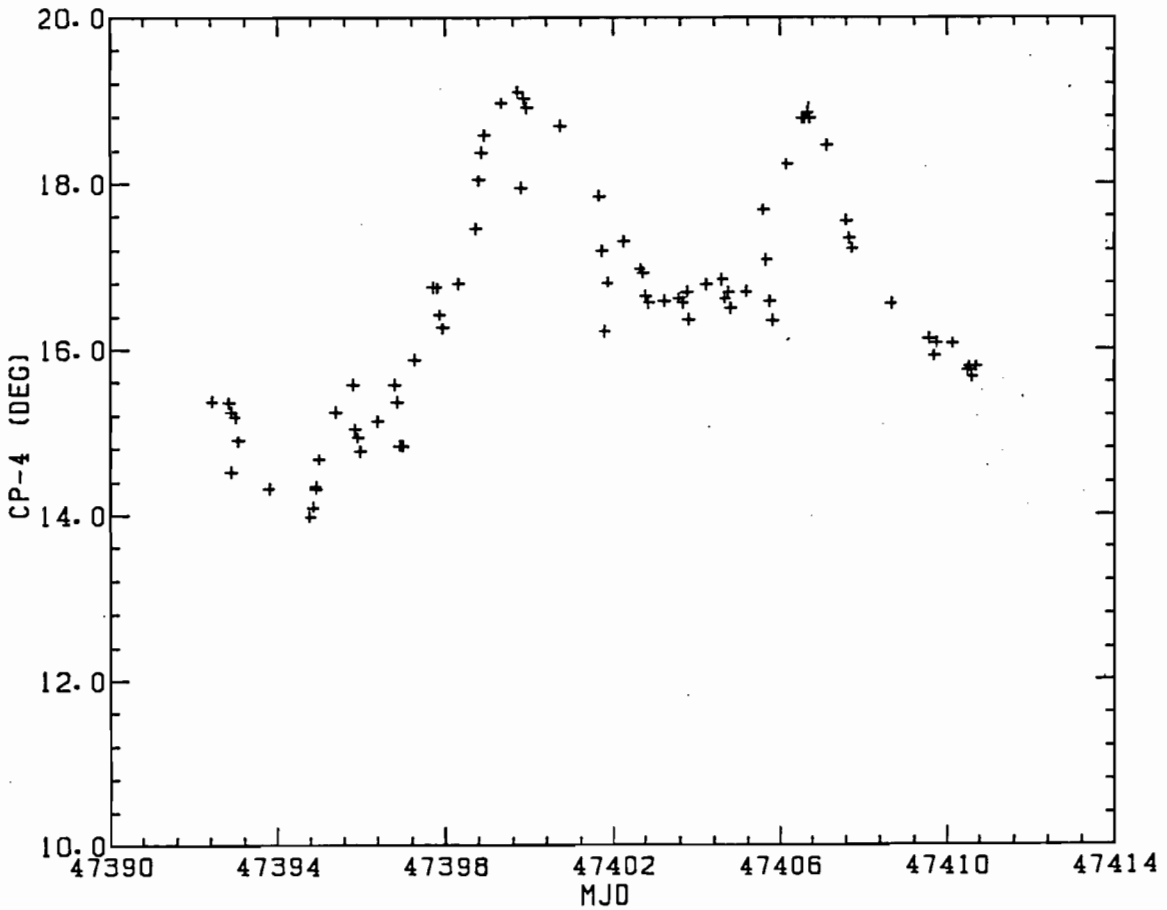
20.0
18.0
16.0
14.0
12.0
10.0
CP-4 (DEG)
47390
47394
47398
47402
47406
47410
47414
MJD

Fig. 2.

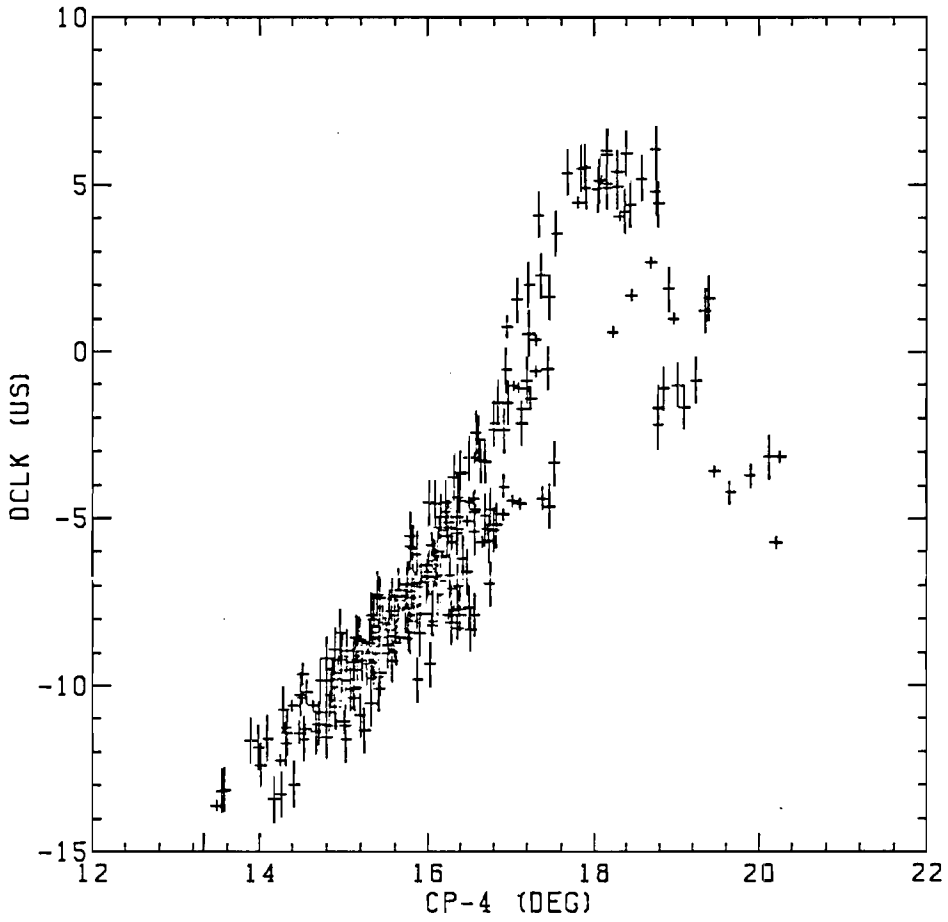
10
5
0
-5
-10
-15
12
14
16
18
20
22
DCLK (US)
CP-4 (DEG)

Fig. 3.

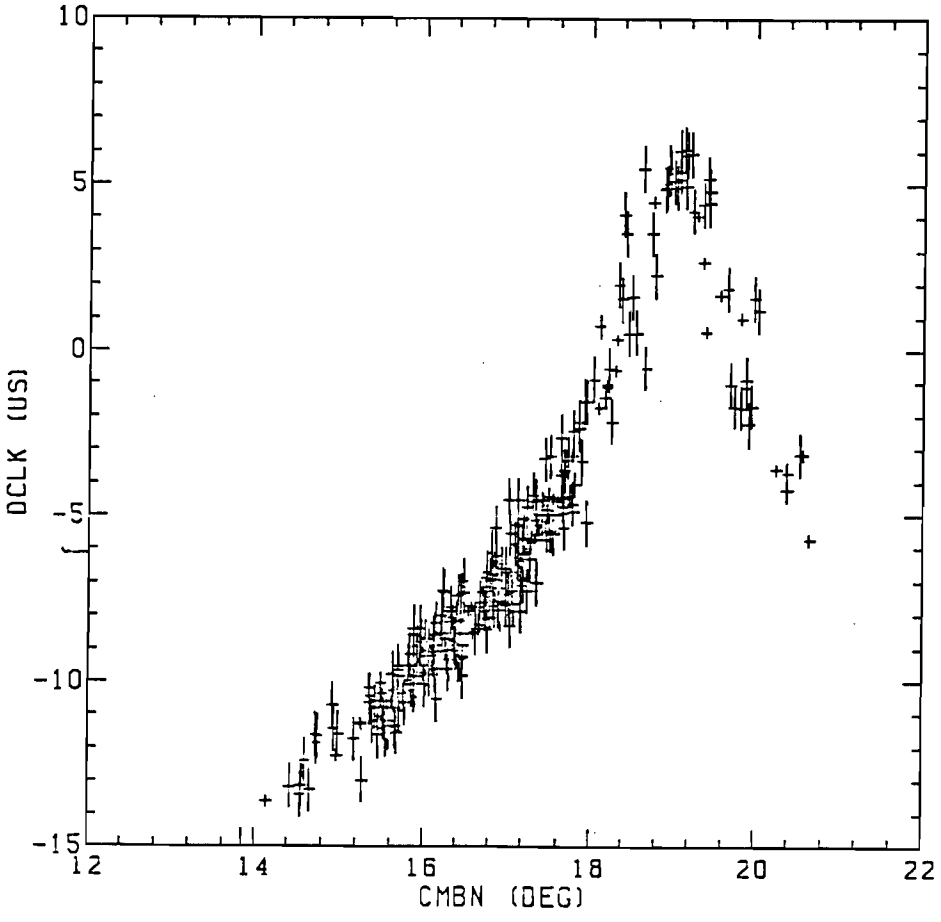
10
5
0
-5
-10
-15
12
14
16
18
20
22
DCLK (US)
CMBN (DEG)

Fig. 4.

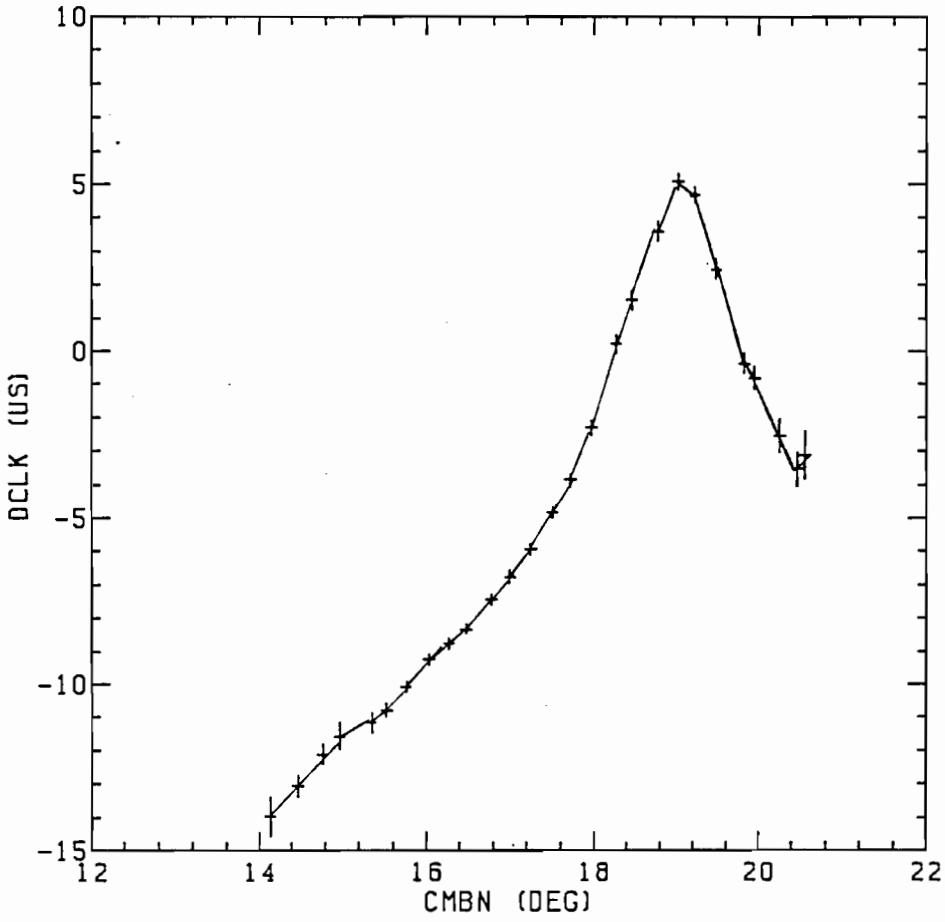
10
5
0
-5
-10
-15
DCLK (US)
12
14
16
18
20
22
CMBN (DEG)

Fig. 5.

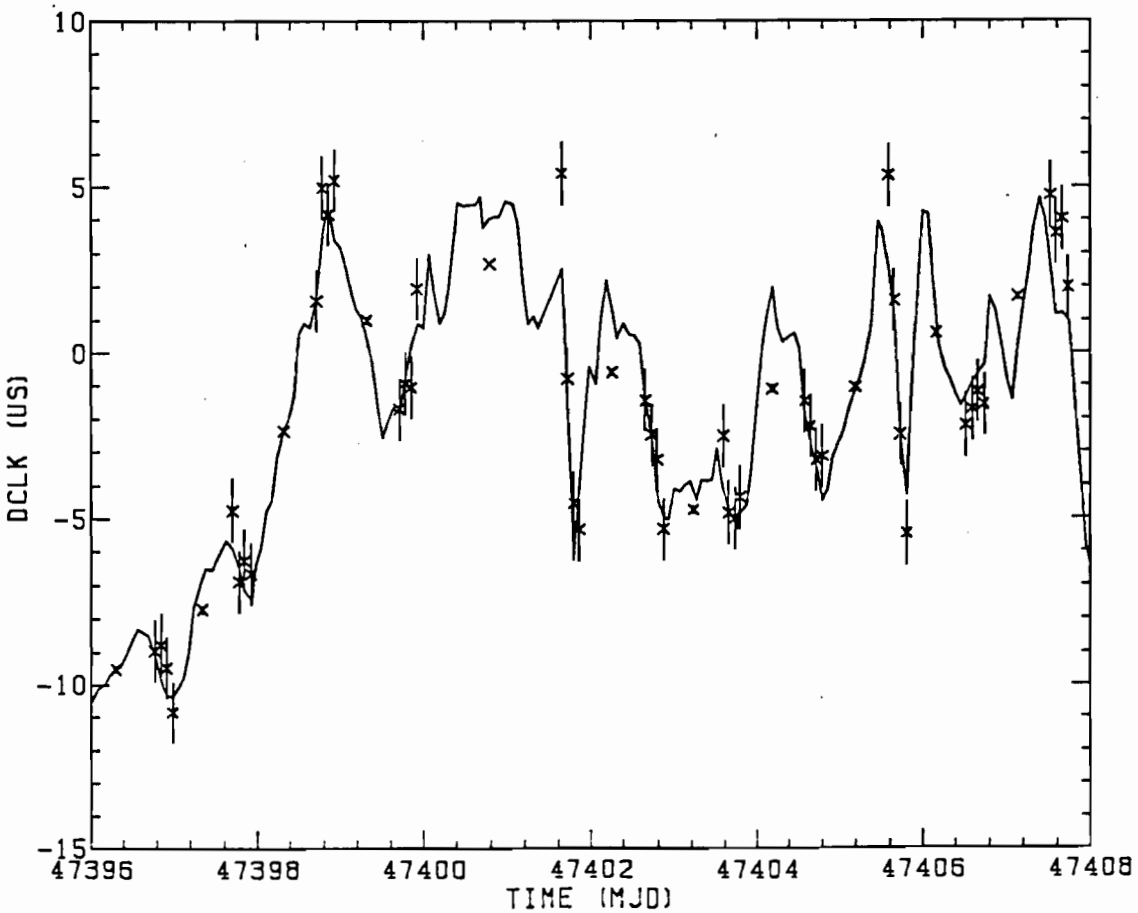
10
5
0
-5
-10
-15
DCLK (US)
47396
47398
47400
47402
47404
47406
47408
TIME (MJD)

Fig. 6.

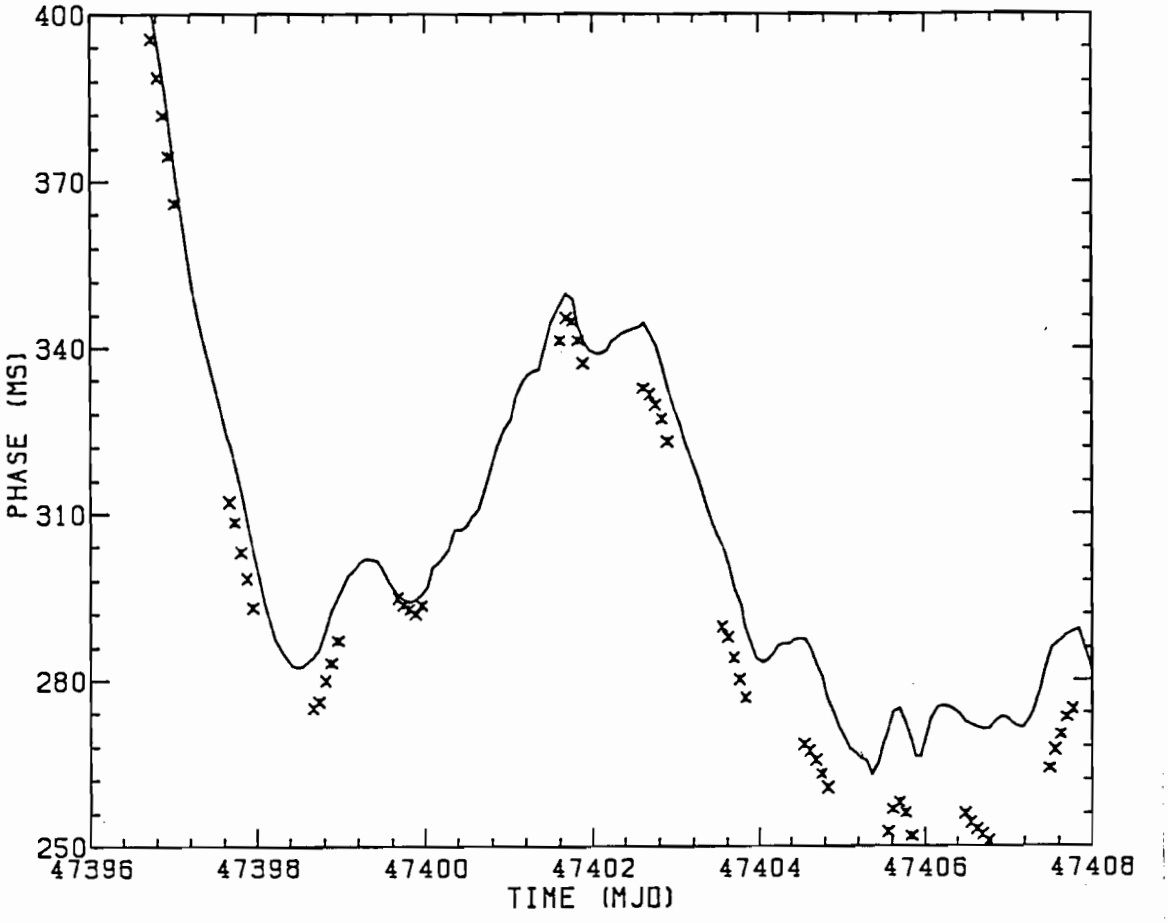
400
370
340
310
280
250
PHASE (MS)
47396
47398
47400
47402
47404
47406
47408
TIME (MJD)

Fig. 7.

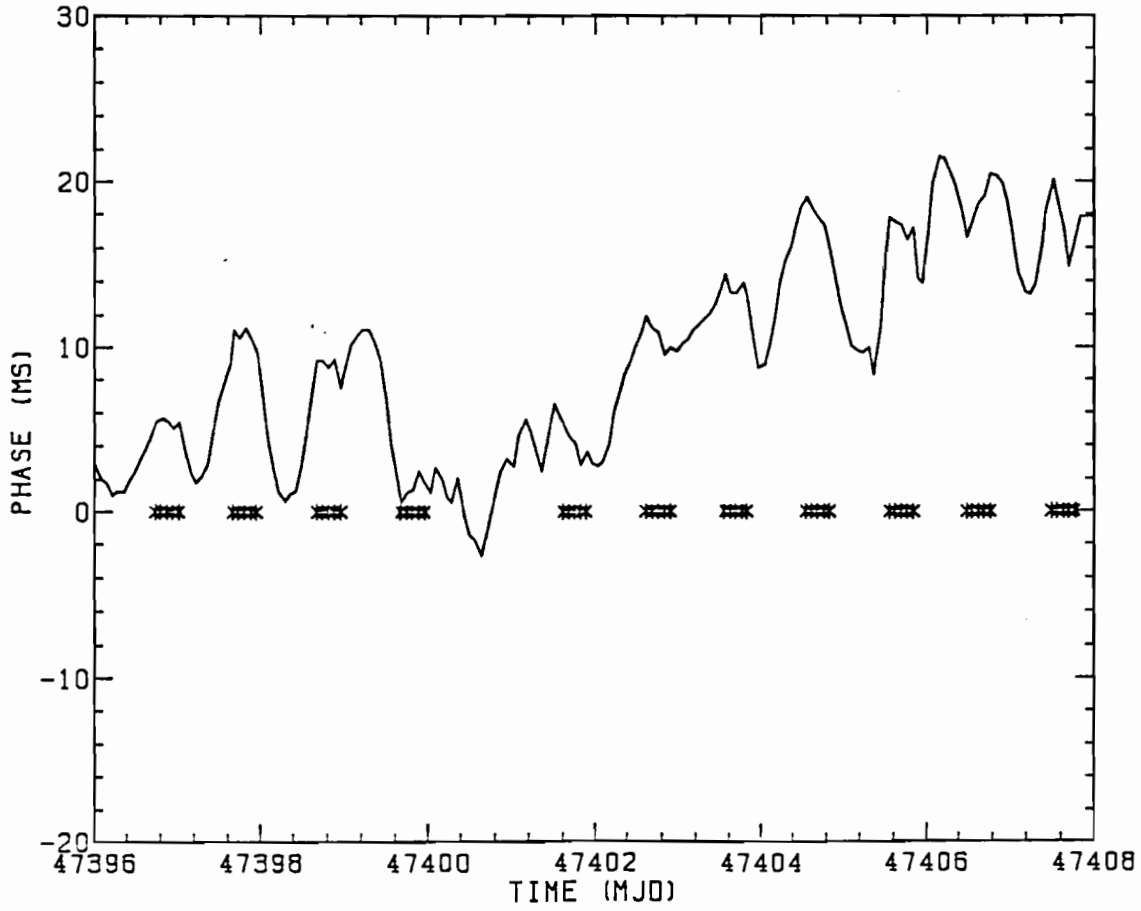
30
20
10
0
-10
-20
PHASE (MS)
47396
47398
47400
47402
47404
47406
47408
TIME (MJD)

Fig. 8.

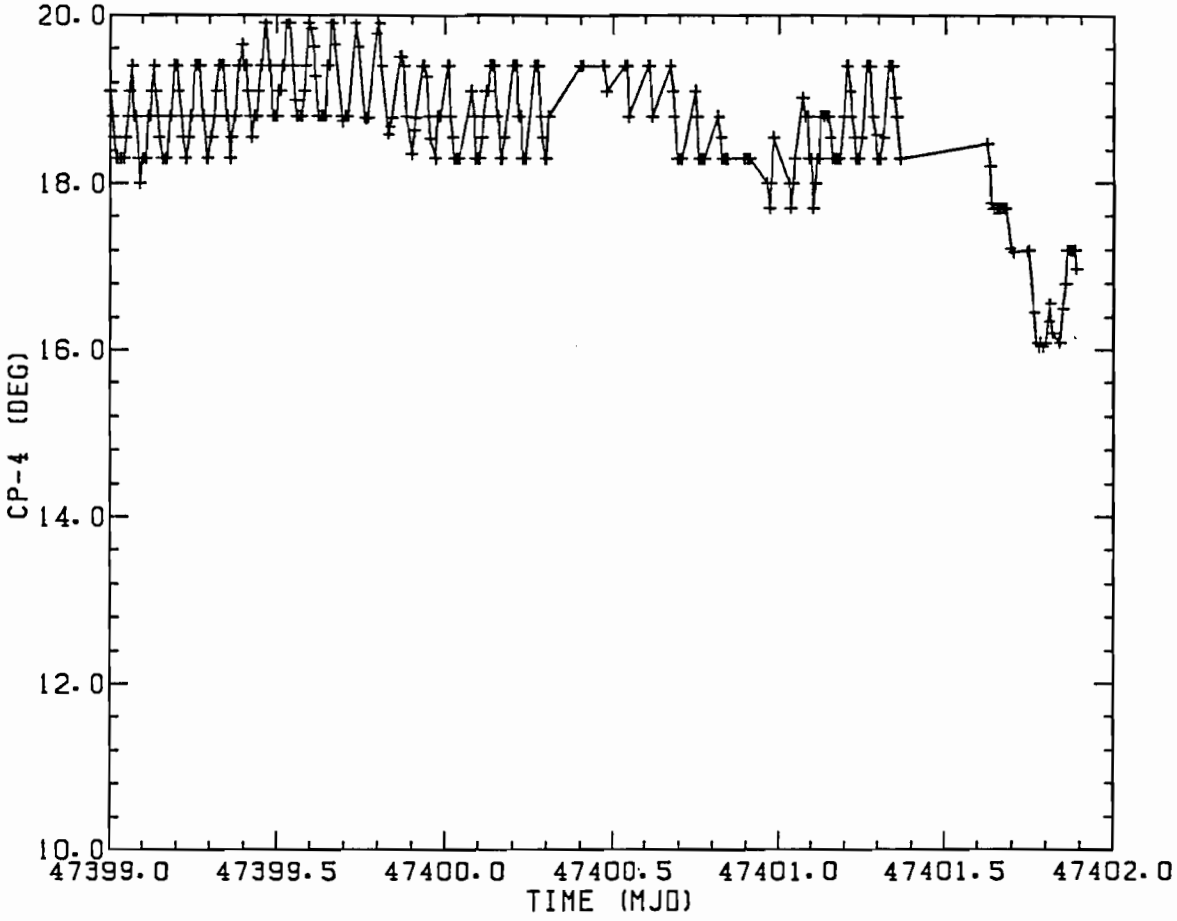
20.0
18.0
16.0
14.0
12.0
10.0
CP-4 (DEG)
47399.0
47399.5
47400.0
47400.5
47401.0
47401.5
47402.0
TIME (MJD)

Fig. 9.

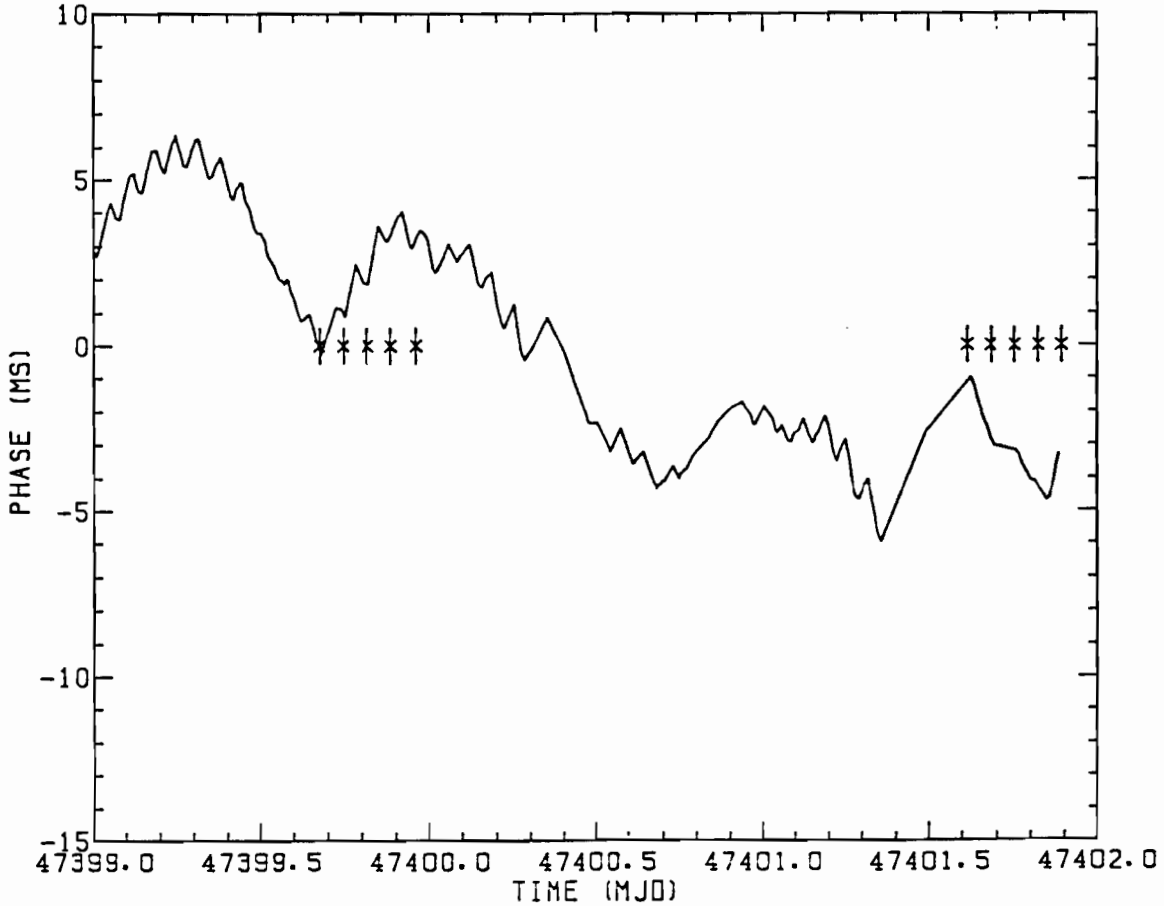
10
5
0
-5
-10
-15
PHASE (MS)
47399.0
47399.5
47400.0
47400.5
47401.0
47401.5
47402.0
TIME (MJD)

Fig. 10.

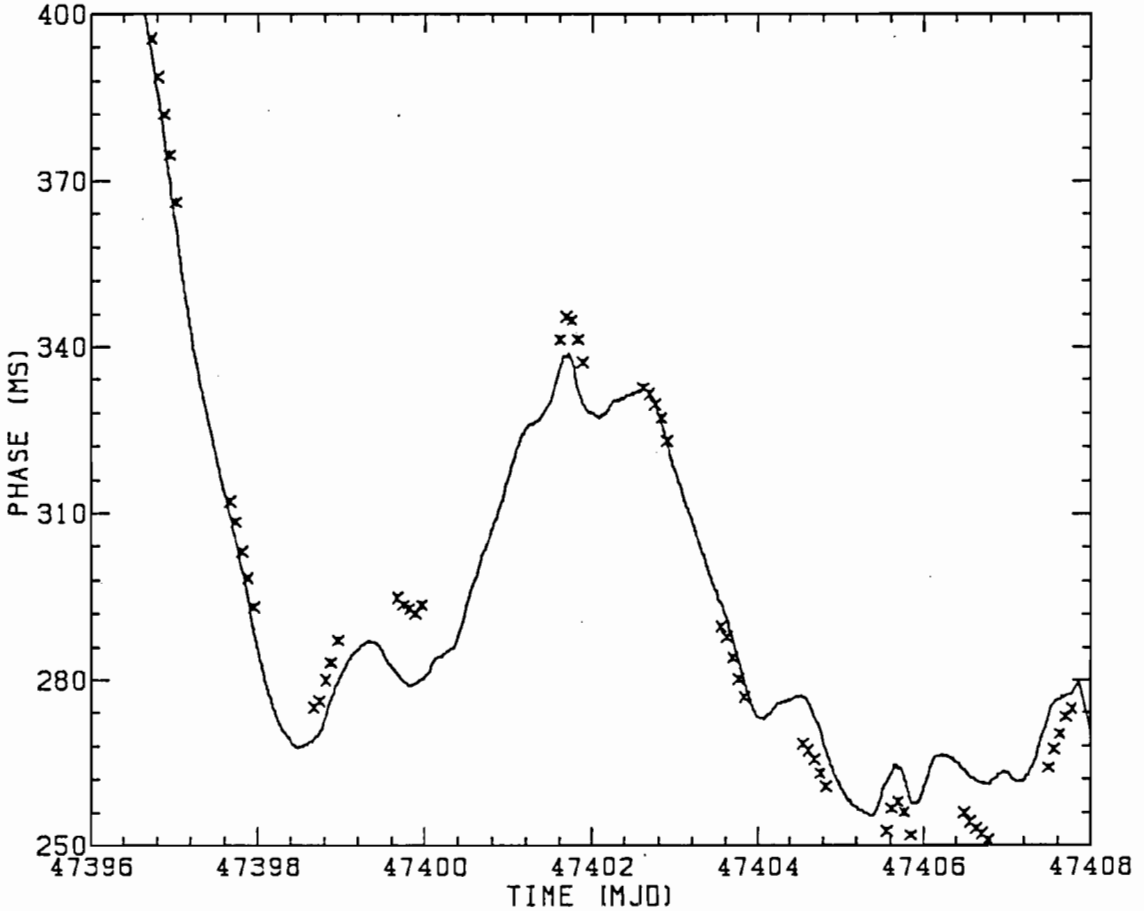
400
370
340
310
280
250
PHASE (MS)
47396
47398
47400
47402
47404
47406
47408
TIME (MJD)

Fig. 11.

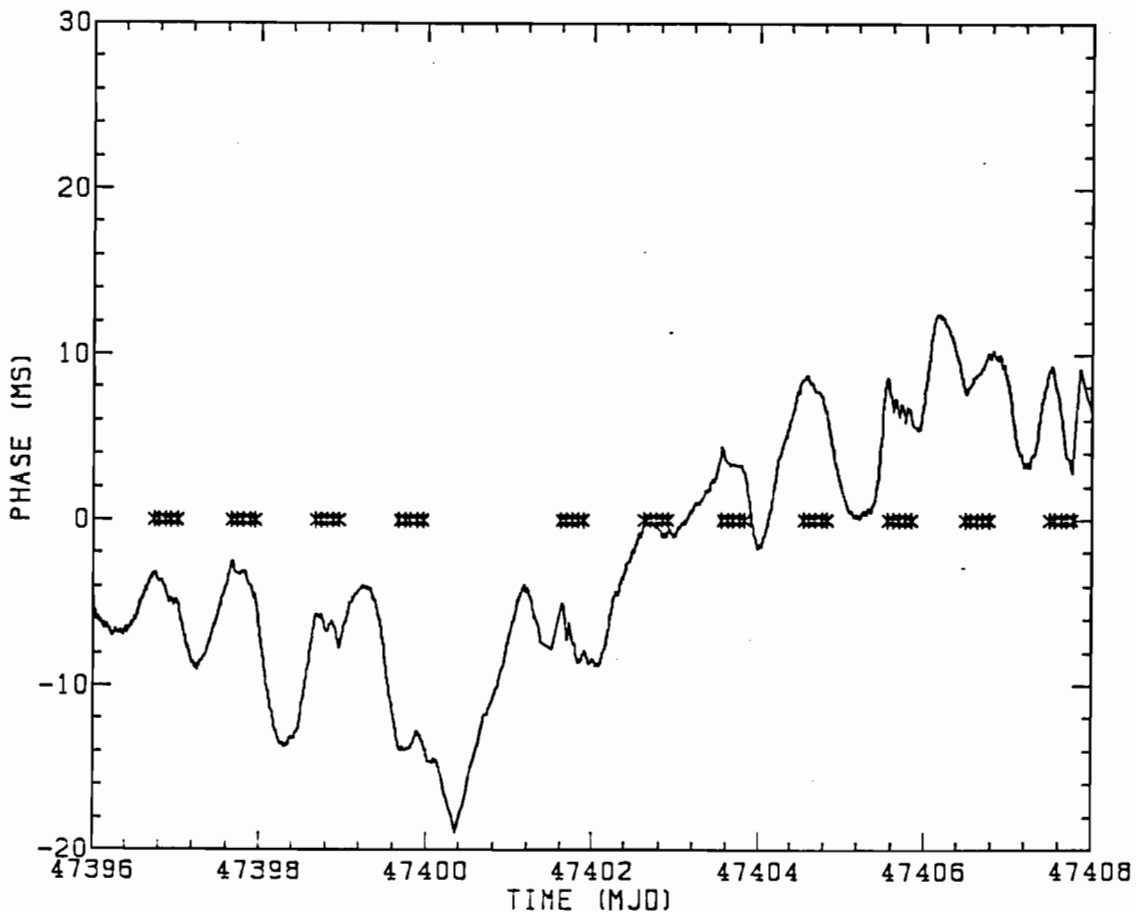
30
20
10
0
-10
-20
PHASE (MS)
47396
47398
47400
47402
47404
47406
47408
TIME (MJD)

Fig. 12.